Rev. Roum. Sci. Techn.– Électrotechn. et Énerg.
Vol. **70**, *4,* pp. 470–476, Bucarest, 2025

MULTI-PHASE PERMANENT MAGNET SYNCHRONOUS MOTOR USING DIRECT TORQUE ADAPTIVE FUZZY CONTROLLED

FAYCAL MEHEDI[1], ISMAIL BOUYAKOUB[1], ABDELKADER YOUSFI[2], ZAKARIA REGUIEG[1]

Keywords: Adaptive fuzzy logic algorithm; Direct torque control; Ripple; Robustness; Five-phase permanent magnet synchronous motor.

The performance of the conventional direct torque control (DTC-C) scheme, which is primarily based on switching tables or conventional proportional integral (PI) controllers, yields high ripples in torque and magnetic flux, thereby compromising the overall robustness of the system. This research proposes an adaptive fuzzy logic control (AFLC) for controlling a five-phase permanent magnet synchronous motor (5P-PMSM), incorporating the space vector modulation (SVM) algorithm. This approach aims to overcome the limitations of DTC-C schemes. The proposed AFLC-DTC-SVM method is designed to enhance the robustness, response time, and efficiency of the 5P-PMSM drive. Simulation results using MATLAB/Simulink demonstrate that the proposed method significantly reduces torque ripple by approximately 72% compared to the DTC-C technique and 51.16% compared to the DTC-SVM method. Flux ripple is also reduced by 71.42% and 33.33% compared to the DTC-C technique and the DTC-SVM method, respectively. Furthermore, the proposed technique offers robust performance against variations in machine parameters and load disturbances, thereby confirming its superiority over conventional methods.

1. INTRODUCTION

Electrical machines that employ more than the traditional three phases often found in ordinary power systems are known as multiphase machines. The potential benefits of these machines, in terms of efficiency, fault tolerance, and dependability, are drawing increasing interest from a variety of industries [1,2]. Due to these advantages, multiphase machines can be utilized in various industries, including multi-machine systems, industrial automation, robotics, electric vehicles, tidal current applications, energy conversion, and aerospace, where performance, fault tolerance, and dependability are crucial [3-5]. Furthermore, multiphase machines are becoming increasingly practical for commercial and industrial applications due to advancements in power electronics and control methods, opening new possibilities for electrical machine design.

A five-phase permanent magnet synchronous motor (5P-PMSM) is a sophisticated electric motor that uses the same synchronous rotational principles as the conventional 3-phase PMSM, but with 5-phase instead. This design enhances several key performance characteristics, including power quality, efficiency, and fault tolerance. By expanding the number of phases, the ripple and harmonics that are commonly observed in lower-phase motors are reduced, and improved torque generation and smoother operation are made possible [6,7].

Advanced techniques are used in the control of 5P-PMSMs to improve fault tolerance, efficiency, and performance in comparison to conventional 3-phase systems. Direct torque control (DTC) and vector control (VC) are some of the methods frequently used to control torque, flux, and speed while guaranteeing steady operation across a range of operating circumstances [8-10]. Nevertheless, even though DTC has numerous benefits, adding a PI regulator to the control loop has several drawbacks: reduced steady-state performance, sensitivity to parameter variations, high switching frequency, high torque ripples, and increased tuning complexity [11].

Recent advancements in control techniques of multiphase motors have highlighted the limitations of traditional DTC with Proportional Integral (PI) controllers. Recent research focuses on developing alternative techniques to achieve better control over torque and flux, resulting in reduced ripple, a consistent switching frequency, and increased robustness. The implementation of a DTC for motors with more than three phases is covered in [12], along with an examination of how other stages affect system performance. Sun *et al.* [13] presented a model predictive (MP) control of the DTC technique for multiphase induction motors with the goal of lowering torque ripple and enhancing overall efficiency. An enhanced DTC method with space vector modulation (SVM) for a 5P-PMSM utilizing sliding mode (SM) speed control was presented in [14]. By combining the accuracy of SVM with the robustness of SM control, the combined method improves performance and resilience to changes in machine parameters. Cao *et al.* [15] described a new DTC technique for multiphase systems that improves efficiency and drastically reduces switching losses. To enhance torque and flux control performance, the extended Kalman Filter is examined and used for direct torque control in polyphase induction motors [16].

Numerous artificial intelligence (AI) techniques have been employed to enhance controller performance, including genetic algorithms (GAs), neural networks (NNs), and fuzzy logic (FL) systems, which have been widely utilized. Each technique improves the effectiveness of controllers and helps to overcome the difficulties associated with manual tuning, particularly in complex and dynamic systems [17,18]. The ANN with DTC has been introduced to reduce the total harmonic distortion (THD) of the 5P-PMSM [19]. A hybrid control strategy that combines FL with DTC to improve torque and flux control in polyphase PMSMs was presented in [20]. In [21], torque ripple issues were addressed by combining a DTC with a PI-based FL optimized by particle swarm optimization.

Additionally, the air-gap harmonics can be significantly reduced by employing the novel space vector pulse width modulation technique. Bellal *et al.* [22] improved the DTC of a multiphase induction motor using an adaptive neuro-fuzzy inference system (ANFIS) and a GA. By improving the torque and flux quality, GA integration increased the

[1] Laboratoire Génie Électrique et Énergies Renouvelables (LGEER), Faculty of Technology, Hassiba Benbouali University of Chlef, Chlef 02000, Algeria.
[2] Laboratory LAGC, Faculty of Science and Technology, Djilali Bounaama University, Khemis Miliana, Algeria.
E-mails: f.mehedi@univ-chlef.dz, i.bouyakoub@univ-chlef.dz, z.reguieg@univ-chlef.dz a.yousfi@univ-bkm.dz

DOI: 10.59277/RRST-EE.2025.70.4.7

machine's dynamic responses.

In this study, an adaptive fuzzy logic control (AFLC) is used to increase the 5P-PMSM's efficiency and provide more accurate and robust control of multiphase machines. This is the paper's original contribution. To demonstrate that the suggested approach offers notable benefits in terms of stability, flux/torque ripples, speed, and robustness, the AFLC-DTC-SVM strategy is applied to 5P-PMSM. The suggested method is compared and examined in the paper alongside other methods, such as SVM-DTC and traditional control DTC-C. This work seeks to further the adaptive fuzzy theory, intelligent control systems, and artificial intelligence algorithms in their applications to multiphase machines.

In this work, Section 2 introduces the DTC approach for the 5P-PMSM. Section 3 presents the DTC with the SVM algorithm of the 5P-PMSM. The AFLC-DTC-SVM strategy for 5P-PMSM is introduced in Section 4. Simulation results are fully presented and summarized in Section 5. and the work is concluded in Section 6.

2. DTC PRINCIPAL OF 5P-PMSM

Traditional DTC offers motors a very effective and responsive control method, but it necessitates real-time processing and precise management of switching frequencies, which can make implementation more challenging [23]. Applying it to a 5P-PMSM provides several benefits because of the additional phase, including decreased torque ripple and enhanced fault tolerance.

In a rotating reference frame (d-q-x-y-o), the 5P-PMSM mathematical model is represented as follows [24]:

A 5P-PMSM stator's voltage state equation is as follows:

$$\begin{aligned} v_{ds} &= R_s i_{ds} + \frac{\mathrm{d}}{\mathrm{d}t}\varphi_{ds} - w_r\varphi_{qs}, \\ v_{qs} &= R_s i_{qs} + \frac{\mathrm{d}}{\mathrm{d}t}\varphi_{qs} + w_r\varphi_{ds}, \\ v_{xs} &= R_s i_{xs} + \frac{\mathrm{d}}{\mathrm{d}t}\varphi_{xs}, \\ v_{ys} &= R_s i_{ys} + \frac{\mathrm{d}}{\mathrm{d}t}\varphi_{ys}, \\ v_{Os} &= R_s i_{Os} + \frac{\mathrm{d}}{\mathrm{d}t}\varphi_{Os}, \end{aligned} \tag{1}$$

where, v_{ds}, v_{qs}, v_{xs} , v_{ys} and v_{os} are the stator voltages in the (d-q,x-y-o) axis, i_{ds}, i_{qs}, i_{xs}, $i_{ys,}$ and i_{os} are the stator currents in (d-q,x-y-o) axis, R_s denotes the stator resistance, φ_{ds}, φ_{qs}, φ_{xs}, φ_{ys} and φ_{os} are the stator flux in the (d-q,x-y-o) axis, w_r denotes the angular speed.

The following is an equation for flow linkages:

$$\begin{aligned} \varphi_{ds} &= L_d i_{ds} + \varphi_f, \\ \varphi_{qs} &= L_q i_{qs}, \\ \varphi_{xs} &= L_{xl} i_{xs}, \\ \varphi_{ys} &= L_l i_{ys}, \\ \varphi_{os} &= L_l i_{os}, \end{aligned} \tag{2}$$

where L_l, L_d, and L_q are the leakage, direct, and quadrature stator inductances, and φ_f is the magnetic flux.

The 5P-PMSM's torque can be expressed as follows:

$$T_{em} = \frac{5}{2}P\left(\left(L_d - L_q\right)i_{ds}i_{qs} + \varphi_f i_{qs}\right). \tag{3}$$

The dynamics equation is:

$$\mathrm{J}_m\frac{\mathrm{d}}{dt}w_r = PT_{em} - PT_r - f_m w_r. \tag{4}$$

where T_r is the load torque, J_m is the inertia, f_m is the viscous damping, *and P* is the number of pairs of poles.

The basic idea of the DTC approach is explained in detail in [8]. By selecting the appropriate voltage vectors, DTC directly controls the flux and torque of the motor. Unlike conventional control systems, which require current loops, this approach enables high precision and dynamic responsiveness.

The Concordia quantities are used to express the stator flux's amplitude as follows:

$$\varphi_s = \sqrt{\varphi_\alpha^2 + \varphi_\beta^2}\,. \tag{5}$$

The stator flux's position θ_s is provided by:

$$\frac{\varphi_\beta}{\varphi_\alpha}. \tag{6}$$

The torque of the 5P-PMSM can be represented as follows in terms of flux, stator and current [14]:

$$T_e = \frac{5}{2}P\left(\varphi_\alpha i_\beta - \varphi_\beta i_\alpha\right). \tag{7}$$

When using DTC, the error between the actual and reference flux and torque is used to determine the voltage vector:

$$\{\Delta\varphi_s = \varphi_s^* - \varphi_s, \quad \Delta T_e = T_{em}^* - T_{em}\,. \tag{8}$$

where, φ_s^* is the reference flux, and T_{em}^* is the reference torque.

To ensure exact control over the 5P-PMSM behavior, the system employs a switching table (ST) to select the appropriate inverter switching states based on the selected voltage vector. Table 1 displays an ST for DTC-C of the 5P-PMSM [19].

Table 1
Switch table for DTC-C

		Sector									
		1	2	3	4	5	6	7	8	9	10
dφ=0	dT= -1	V7	V3	V19	V17	V25	V24	V28	V12	V14	V6
	dT= 0	V31	V0	V31	V0	V31	V0	V31	V0	V31	V0
	dT= 1	V14	V6	V7	V3	V19	V17	V25	V24	V28	V12
dφ =1	dT= -1	V17	V25	V24	V28	V12	V14	V6	V7	V3	V19
	dT= 0	V0	V31	V0	V31	V0	V31	V0	V31	V0	V31
	dT= 1	V24	V28	V12	V14	V6	V7	V3	V19	V17	V25

3. DTC-SVM TECHNIQUE

Conventional DTC doesn't optimize switching states, leading to high losses and torque ripple due to voltage vector selection based solely on flux and torque errors. However, SVM offers a sophisticated alternative for inverter switching signals [19].

To enhance the 5P-PMSM traditional DTC performance, we provide a novel DTC control strategy based on the SVM approach in this section. In contrast to the VC and DTC-C, the DTC-SVM approach minimizes stator flux ripple, torque ripple, and uses simple schemes.

Figure 1 (a) shows the active vectors of the α-β frame, while Fig. 1 (b) represents the active vectors of the x-y frame [14]. There are 2 or 4 vector techniques of applying the 5-

phase SVM. There are 3 groups that comprise the active switching vectors: medium, large, and small switching vectors.

The following is the formula for switching time when utilizing the 4-vector technique:

$$V_s^* T_s = V_{al} T_{al} + V_{al} T_{bl} + V_{bl} T_{am} + V_{bm} T_{bm} . \quad (9)$$

Where, V_s^* reference voltage vector; T_s switching period; T_{am}, T_{bm}, T_{al}, and T_{bl} the switching time of medium and long voltage vectors (V_{am}, V_{bm}, V_{al}, and V_{bl}); V_{dc} denote DC voltage source.

$$|V_{al}| = |V_{bl}| = |V_l| = \frac{2}{5} V_{dc} 2 \cos\cos\left(\frac{\pi}{2}\right)$$

$$|V_{am}| = |V_{bm}| = |V_m| = \frac{2}{5} V_{dc}, \quad (10)$$

$$\frac{T_{al}}{T_{am}} = \frac{T_{bl}}{T_{bm}} = \frac{V_l}{V_m} = \tau = 1.618. \quad (11)$$

Equations (9), (10), and (11) can be solved to get the equation for the switching time [14].

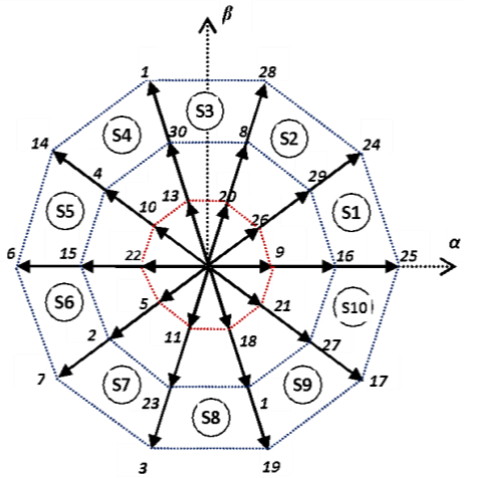

(a)

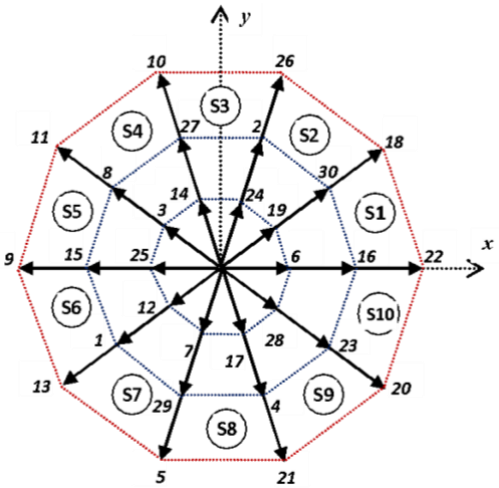

(b)

Fig. 1 – The voltage space vectors and the switching states of the 5-phase inverter in: (a) α-β frame, (b) x-y frame.

Figure 2 provides the block diagram for the DTC-SVM method of the 5P-PMSM.

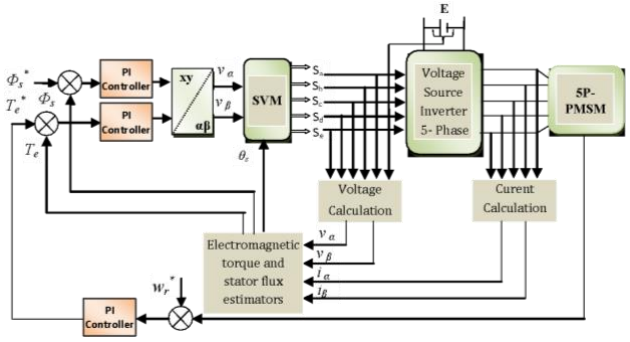

Fig. 2 – Synoptic schema of DTC-SVM approach control of the 5P-PMSM.

4. THE AFLC-DTC-SVM STRATEGY OF THE 5P-PMSM

Traditionally, 5P-PMSM is controlled by DTC using PI controllers. When using PI controllers, certain drawbacks exist. This method increases torque ripples, which reduces the system's robustness [14].

4.1. DTC BASED ON FL CONTROLLER

Applying fuzzy logic theory to systems that are defined mathematically, complex systems, and physical events with precise mathematical models has made it a very active field of study. Decision-making and the linguistic method form the foundation of this theory. Therefore, the intended controller needs an algorithm that enables the transformation of the expert-based linguistic control strategy into a machine control technique [25–27].

Typically, the linguistic variables in an FL are usually the error *e*, the variation of the order Δ*u*, and the variation of this error *Δe*. The Membership Functions (MF) of the linguistic variables that represent Δ*u*, Δ*e*, and *e* are practically contained in the database. In this study, as shown in Figs. 3 and 4, we have limited the Δ*u* at the interval [-10, 10] and the universes of the discourse of the Δ*e* and *e* at the interval [-1, 1]. The MFs are separated into seven fuzzy groups. The 49 FL rules are displayed in Table 2.

Table 2

The FL rule base

		e_k						
		NS	NB	NM	EZ	PM	PB	PS
Δe_k	NS	NM	NG	NG	NS	PS	PM	EZ
	NM	NG	NB	NG	NM	EZ	PS	NS
	NB	NB	NB	NB	NB	NS	EZ	NM
	EZ	NS	NG	NM	EZ	PM	PB	PS
	PB	PM	EZ	PS	PB	PB	PB	PB
	PM	PS	NS	EZ	PM	PB	PB	PB
	PS	EZ	NM	NS	PS	PB	PB	PM

Negative medium (NM), Positive Small (PS), equal zero (EZ), positive big (PB), negative small (NS), positive medium (PM), and negative big (NB) are the fuzzy labels that are employed in this approach.

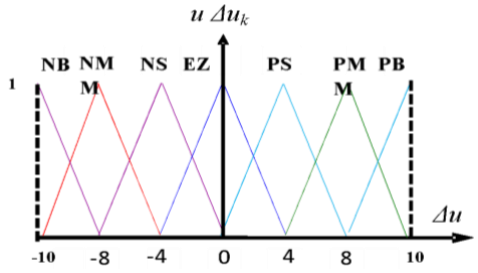

Fig. 3 – MFs of the order variation.

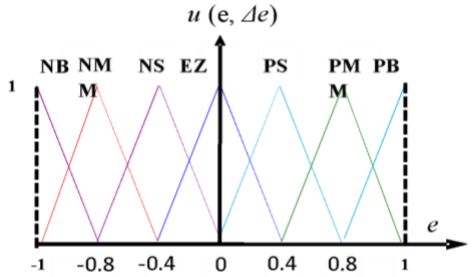

Fig. 4 – Error MF and error variation.

4.2. ADAPTIVE GAIN BLUR CONTROLLER

The gain associated with the control's variation is assumed to be constant in the literature on fuzzy control. Nevertheless, this lengthens the system's response time.

A decision table for the gain is necessary to address this issue and improve the system's dynamic performance, as shown in Table 3. Its variation from time t_k to time t_{k+1} is derived from the control decision table by:

$$u_{k+1} = u_k + G_{\Delta u_{k+1}} + \Delta u_{k+1} . \quad (12)$$

The goal of variable gain in this method is to guarantee sufficient system stability and modify the FL algorithm according to each system scenario. Consequently, we need to consider the gain as a fuzzy variable, requiring the definition of several fuzzy sets. Every fuzzy control set has a corresponding fuzzy gain set, which is always strictly positive but of the same kind (see Table 3). Figure 5 shows the corresponding MF for the fuzzy set with the adaptive gain that we selected.

Table 3

The gain fuzzy control rules

		e						
		NS	NB	NM	EZ	PM	PS	PB
Δe	NS	PS	PB	PM	PVS	PVS	PVS	PP
	NM	PM	PVB	PB	PS	PVS	PVS	PVS
	NB	PB	PVB	PVB	PM	PVS	PS	PVS
	EZ	PVS	PM	PS	PVS	PS	PVS	PM
	PB	PS	PVS	PVS	PM	VB	PB	PVB
	PM	PVS	PVS	PVS	PP	PB	PM	PVB
	PS	PSV	PS	PVS	PVS	PM	PS	PB

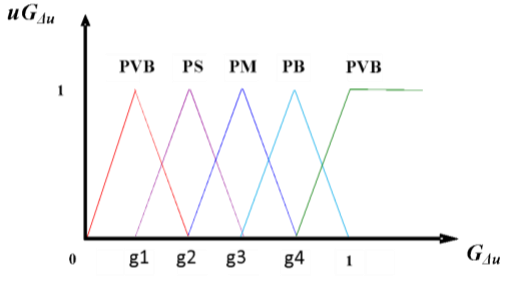

Fig. 5 – The control's gain MF.

The FL with adaptive control gain is described in the following schematic (Fig. 6). We use the designed controllers to show the precision of the developed process with the machine parameters and to monitor the induction command. Where: y represents the stator currents i_{ds} and i_{qs} and speed w_r for the 5P-PMSM.

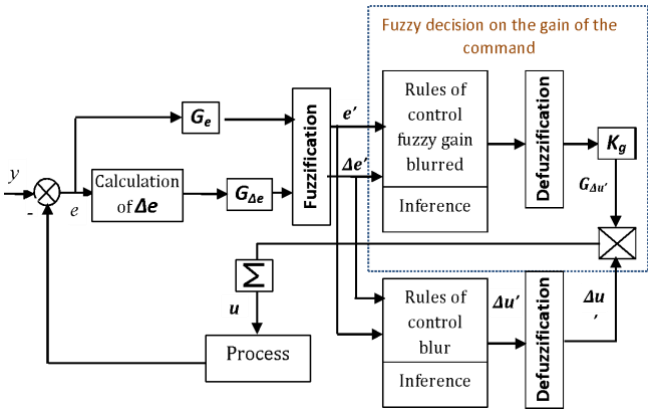

Fig. 6 – An adaptive gain fuzzy controller schematic.

5. SIMULATION RESULTS

MATLAB/Simulink is utilized in this work to simulate the results of the proposed control technique under the DTC scheme using the AFLC-based SVM algorithm for the 5P-PMSM. All the 5P-PMSM characteristics are listed in Table 4 [28].

Table 4

Parameters of the 5P-PMSM

Parameters	Value
Nominal power P_n	1.5 Kw
Number of pairs poles P	2
Stator resistance R_S	0.67 Ω
Direct stator inductance L_d	0.0085 H
Leakage stator inductance L_l	0.00093 H
Quadrature stator inductance L_q	0.0085 H
DC Bus Voltage V_{dc}	400 V
Moment of inertia J_m	0.004 kg/m2

The effectiveness of the control method has been assessed using two test categories. In the first test, the efficiency of the suggested controller under tracking performance and sensitivity to load torque T_r fluctuation is examined by a comparison analysis with an AFLC technique. The second test verifies the robustness of the suggested control strategy, considering the variation of 5P-PMSM parameters.

5.1. TRACKING PERFORMANCE

The purpose of this test is to examine how the suggested AFLC technique of the DTC diagram for 5P-PMSM control behaves when tracking references under the influence of T_r variation. The reference speed of the 5P-PMSM is set to 750 rpm upon startup. At t = 0.2 s, the rotor speed increases to 1250 rpm. In the time t = [0.4, 0.6 s], a nominal T_r = 10 N·m was applied, followed by a consign inversion (-250 rpm) at t = 0.8 s. Fig. 7 displays the simulation results for the rotation speed. According to the simulation findings, the rotor speed follows its reference for all three control types. The suggested control strategy, AFLC-DTC-SVM, however, performs better at tracking rotor speed. When compared to DTC-SVM and DTC-C, the suggested control reaction time is very fast. Additionally, a rejection of speed disturbances (approximately 3% of the AFLC-DTC-SVM strategy): Fig. 8 displays the torque temperature simulation results. The T_{em} ends the

transitory state by returning to 0 N·m. Regarding the suggested DTC technique, we also note that when a T_r is introduced at $t = 0.2$ s, the torque matches its reference value and decreases the ripple torque compared to DTC-SVM and DTC-C, where the torque T_{em} ripple values reach 4.3 N·m and 7.5 N·m, respectively.

The stator flux was improved using the proposed technique in Fig. 9, resulting in a very low ripple (0.004 Wb) compared to conventional methods. The flux ripple values reached 0.006 Wb and 0.014 Wb using methods DTC-SVM and DTC-C, respectively (see Table 5).

Table 6 represents the value of the reduction ratio (RR) of the torque/ flux ripples. An analysis of Table 6 reveals that the AFLC-DTC-SVM approach outperformed both the DTC-C and DTC-SVM techniques in terms of reducing torque and flux ripples. The torque ripple reduction ratio (RR) was improved by approximately 72% over DTC-C and 51.16% over DTC-SVM. Furthermore, stator flux ripple saw reductions of 71.42% and 33.33% when compared to the DTC-C and DTC-SVM methods, respectively. The flux trajectories of the proposed AFLC-DTC-SVM method in Fig. 10 show a significant reduction.

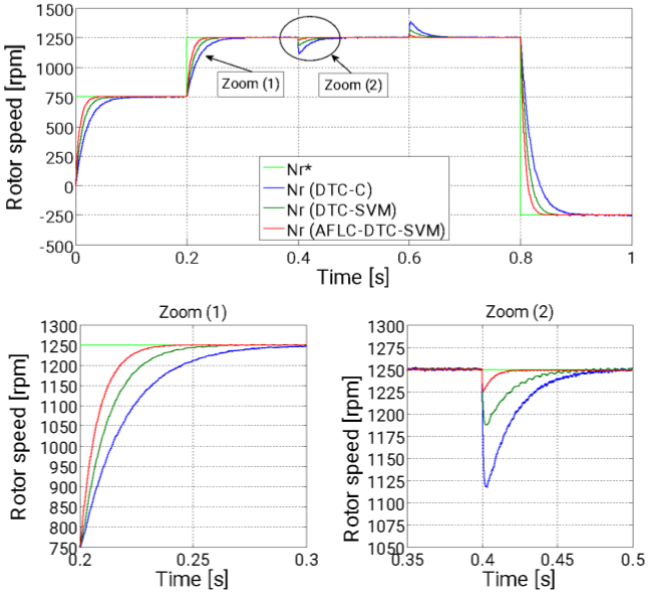

Fig. 7 – Rotation speed.

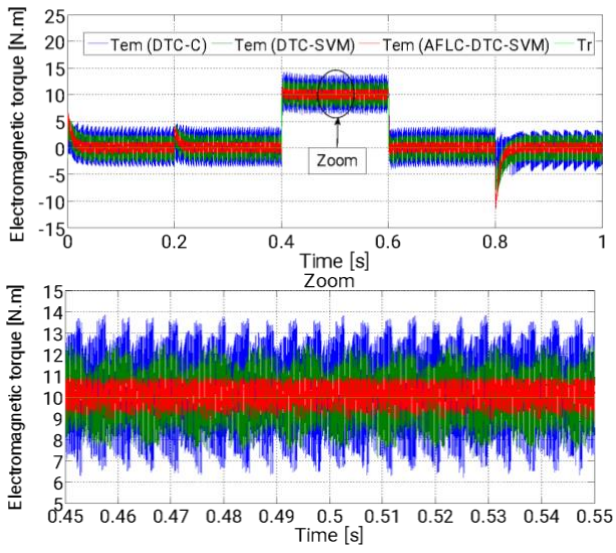

Fig. 8 – Electromagnetic torque.

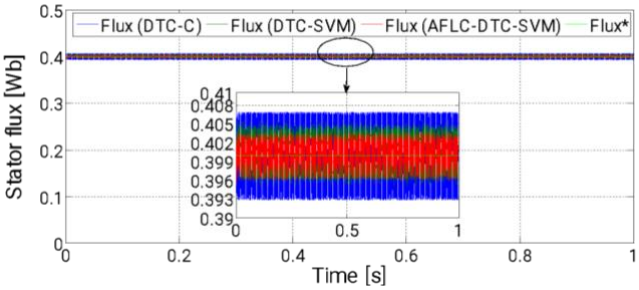

Fig. 9 – Rotor flux.

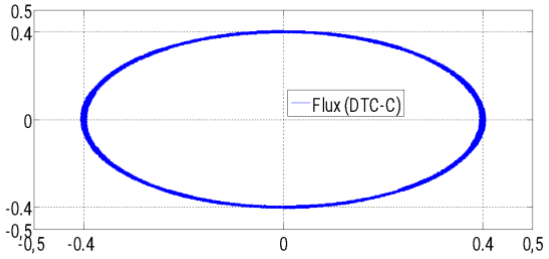

(a)

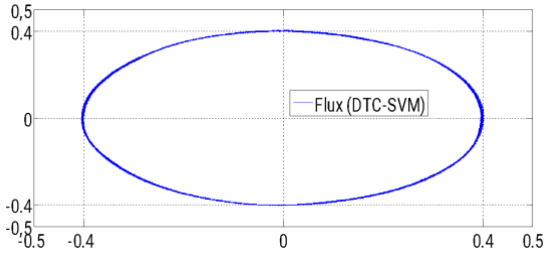

(b)

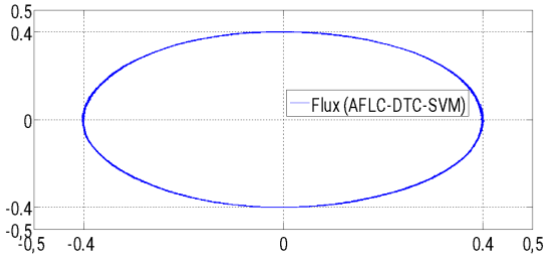

(c)

Fig. 10 – Stator flux trajectories in α-β axis when: (a) DTC-C, (b) DTC-SVM, (c) AFLC-DTC-SVM.

From these results, it can be concluded that the AFLC-DTC-SVM control methods for 5P-PMSM exhibit excellent tracking performance in the test.

Table 5

The Comparative analysis of the various techniques

	DTC-C	DTC-SVM	AFLC-DTC-SVM
N_r response time [s]	0.30 s	0.25 s	0.23 s
Torque ripples [N.m]	6.3-13.8	7.8-12.1	8.9-11
N_r dropping due to T_r application [rpm]	1120	1185	1233
Flux ripples [Wb]	0.393-0.407	0.397-0.403	0.398-0.402

The ratios mentioned in Table 6 were estimated using the reduction ratio (RR) of the torque ripple (RR_{torque}) and flux ripple (RR_{flux}) given by eq. (13)-(16):

$$RR1_{torque}(\%) = \frac{T_{S1}-T_{S3}}{T_{S1}}, \quad (13)$$

$$RR2_{torque}(\%) = \frac{T_{S2}-T_{S3}}{T_{S2}}, \quad (14)$$

$$RR1_{flux}(\%) = \frac{F_{S1}-F_{S3}}{F_{S1}}, \quad (15)$$

$$RR2_{flux}(\%) = \frac{F_{S2}-F_{S3}}{F_{S2}}, \quad (16)$$

where T_{S1}, T_{S2}, $F_{S1,}$ and F_{S2} represent the fluctuation values for the torque and stator flux of the DTC-C (S1), DTC-SVM (S2). T_{S3} and F_{S3} represent the fluctuating values for the torque and stator flux of the AFLC-DTC-SVM (S3).

Table 6

The reduction ratio of the torque/flux ripples

	Torque ripples	Flux ripples
DTC-C	7.5 N·m	0.014 Wb
DTC-SVM	4.3 N·m	0.006 Wb
AFLC-DTC-SVM	2.1 N·m	0.004 Wb
$RR1_{torque}$	72 %	/
$RR2_{torque}$	51.16 %	/
$RR1_{flux}$	/	71.42 %
$RR2_{torque}$	/	33.33 %

5.2. Test of the Robustness (TR)

The robustness of the proposed control system was evaluated for three major variations of 5P-PMSM parameters. The nominal value of stator inductance L_q and L_d was reduced by 20 %, and the value of J_m inertia moment and stator resistance R_s was increased by 100 %. The simulation's outcomes are shown in Figs 11–13. The SVM-DTC and DTC-C speed responses are more affected by inertia changes than the AFLC-DTC-SVM for the 5P-PMSM, according to the results displayed in Fig. 11. We can therefore conclude that the latter is less susceptible to this type of parameter fluctuation. These variations in machine parameters have an obvious influence on the torque, T_{em}, stator flux, and w_r response using the conventional DTC-C and DTC-SVM, where the torque ripple values reached 11.4 N·m and 5.3 N·m, respectively (see Fig. 12). Flux ripple values reached 0.022 Wb and 0.011 Wb, respectively (see Fig. 13). While we did not observe such an influence using the proposed AFLC-DTC-SVM method for the 5P-PMSM.

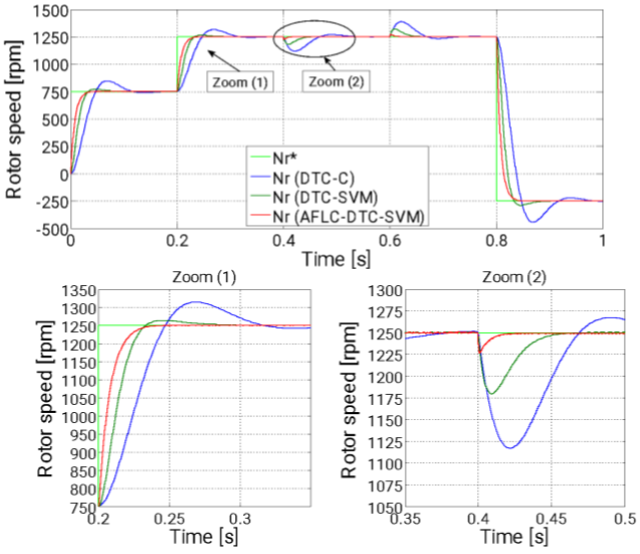

Fig. 11 – Rotation speed (TR).

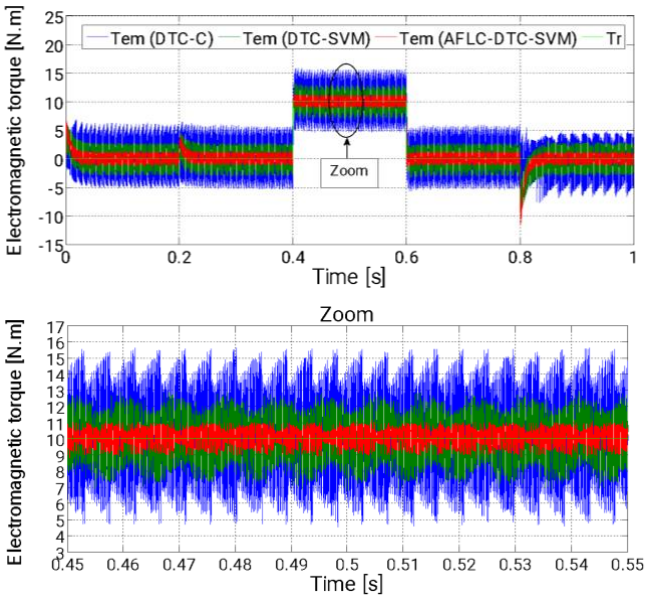

Fig. 12 – Electromagnetic torque (TR).

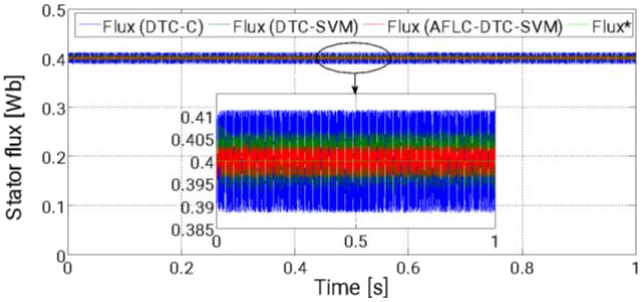

Fig. 13 – Rotor flux (TR).

6. CONCLUSIONS

This study presents a robust control for the DTC scheme utilizing the SVM method, which is based on the adaptive fuzzy logic control technique. This suggested technique, AFLC-DTC-SVM, is applied to the 5P-PMSM drive. In comparison to the DTC strategy based on the DTC with PI controller and DTC classical, the simulation results show that the AFLC controller for the DTC–SVM technique has a satisfactory performance for a 5P-PMSM drive in terms of reference tracking for every control loop, reduces ripple torque and flux, improves response time, and has good robustness against changes in machine parameters.

Future research will suggest further novel and highly effective methods, like hybrid algorithm nonlinear approaches with artificial intelligence algorithms. Furthermore, this study will be tried experimentally and verified by the simulated outcomes that are obtained.

CREDIT AUTHORSHIP CONTRIBUTION STATEMENT

Fayçal Mehedi: writing – review & editing, writing – original draft, visualization, validation, software, methodology, investigation, formal analysis, data curation, conceptualization.

Ismail Bouyakoub: writing – review & editing, writing – original draft, visualization, validation, supervision, software, project administration, methodology, data curation, conceptualization.

Abdelkader Yousfi: writing – original draft, visualization, validation, supervision, software, resources, project administration, methodology, investigation, formal analysis, data curation, conceptualization.

Zakaria Reguieg: writing – original draft, visualization, validation, software, resources, project administration, methodology, investigation, formal analysis, data curation, conceptualization.

Received on 31 December 2024

REFERENCES

1. Y. Xia, B. Ren, B. Jing, Z. Chen, *Analysis of transient temperature field of five-phase induction motor with composite winding under different operating conditions*. Case Studies in Thermal Engineering, **63**, pp. 105402 (2024).
2. A. Zeghlache, H. Mekki, M.F. Benkhoris, A. Djerioui, D. Ziane, S. Zeghlache, *Robust fault-tolerant control of a five-phase permanent magnet synchronous motor under an open-circuit fault*, Appl. Sci., **14**, pp. 5190 (2024).
3. A. Muc, M. Morawiec, F. Wilczyński, *Steady-state vibration level measurement of the five-phase induction machine during third harmonic injection or open-phase faults*, Energies, **16**, *2*, pp. 838 (2023).
4. S. Sahu, B. Nayak, R.N. Dash, *Modeling and analysis of five-phase surface PMSM for application in electric vehicle*, Journal of Electrical Systems, **18**, *1*, pp. 62–68 (2024).
5. A. Z. Liu, A. Houari, M. Machmoum, M.F. Benkhoris, F.A. Djerioui, T. Tang, *Experimental investigation of a real-time singularity-based fault diagnosis method for five-phase PMSG-based tidal current applications*, ISA Transactions, **142**, *4*, pp. 501–514 (2023).
6. S Mo, D. Ziane, M Oukrid, M.F. Benkhoris, N. Bernard, *Dynamic modeling approach in view of vector control and behavior analysis of a multi-three-phase star permanent magnet synchronous motor Drive*, Energies, **17**, *7*, pp. 1567 (2024).
7. M. Oukrid, N. Bernard, M.F. Benkhoris, D. Ziane, *Design and optimization of a five-phase permanent magnet synchronous machine exploiting the fundamental and third harmonic*, Machines, **12**, *2*, pp. 117 (2024).
8. N. Bounasla, S. Barket, *Constant switching frequency predictive direct torque control of a five-phase PMSM*, International Journal of System Assurance Engineering and Management, **13**, pp. 772–782 (2022).
9. W. Huang, Y. Barket, D. Xu, *Model-free predictive current control of five-phase PMSM drives*, Electronics, **12**, *23*, pp. 4848 (2023).
10. P. Rajanikanth, M.L. Parvathy, V.K. Thippiripati, *Enhanced model predictive current control-based five-phase PMSM drive*, IEEE Journal of Emerging and Selected Topics in Power Electronics, **12**, *1*, pp. 838–848 (2024).
11. N. Bounasla, S. Barkat, *Optimum design of fractional order PIα speed controller for predictive direct torque control of a sensorless five-phase permanent magnet synchronous machine (PMSM)*, Journal Européen des Systèmes Automatisés (JESA)., **53**, *4*, pp. 437–449 (2020).
12. V. Rathore, K.B. Yadav, *Direct torque control of asymmetrical multiphase (6-phase) induction motor using modified space vector modulation*, Recent Advances in Power Electronics and Drives., **707**, pp. 9–45 (2021).
13. X. Sun, X. Lin, L. Zhang, Y. Cai, *An improved torque enhancement strategy for dual three-phase PMSM based on model-free predictive current control*, IEEE Transactions on Transportation Electrification, (2024).
14. F. Mehedi, R. Taleb, D.A. Belhadj, A. Yahdou, *SMC-based DTC-SVM control of five-phase permanent magnet synchronous motor drive*, Indonesian Journal of Electrical Engineering and Computer Science, **20**, *1*, pp. 100–108 (2020).
15. B. Cao, B.M. Grainger, X. Wang, Y. Zou, G.F. Reed, Z.H. Mao, *Direct torque model predictive control of a five-phase permanent magnet synchronous motor*, IEEE Transactions on Power Electronics, **36**, *2*, pp. 2346–2360 (2021).
16. A. Taheri, H.P. Ren, C.H. Song, *Sensorless direct torque control of the six-phase induction motor by fast reduced order extended Kalman Filter*, Complexity, **1**, pp. 1–10 (2020).
17. M.I. Abdelwanis, R.A. Sehiemy, M.A. Hamida, *Hybrid optimization algorithm for parameter estimation of poly-phase induction motors with experimental verification*, Energy AI, **5**, 100083, pp. 1–15 (2021),
18. R.E.S. Mohamed I. Abdelwanis, *Efficient parameter estimation procedure using sunflower optimization algorithm for six-phase induction motor*, Rev. Roum. Sci. Techn.–Électrotechn. et Énerg., **67**, *3*, pp. 259–264, 2022.
19. F. Mehedi, H. Benbouhenni, L. Nezli, D. Boudana, *feedforward neural network-DTC of multi-phase permanent magnet synchronous motor using five-phase neural space vector pulse width modulation strategy*, Journal Européen des Systèmes Automatisé (JESA), **15**, *3*, pp. 345–354 (2021).
20. N.M. Max, N.Y.J. Maurice, E. Samue, M.J. Jordan, A. Biboum, B. Laurent, *DTC with fuzzy logic for multi-machine systems: traction applications*, International Journal of Power Electronics and Drive Systems (IJPEDS), **12**, *4*, pp. 2044–2058 (2021).
21. K. Belalia, A. Mostefa, H.M. Boulouiha, A. Draou, M. Denai, *Direct torque control of a dual star induction generator based on a modified space vector PWM under fault conditions*, ISA Transactions, **155**, pp. 237–260 (2024).
22. R. Bellal, M Flitti, M.L. Zegai, *Tuning of Pi speed controller in direct torque control of dual star induction motor based on genetic algorithms and neuro-fuzzy schemes*, Rev. Roum. Sci. Techn. – Électrotechn. Et Énerg., **69**, *1*, pp. 9–14 (2024).
23. E. Benyoussef, S. Barkat, *Three-level direct torque control based on balancing strategy of five-phase induction machine*, Rev. Roum. Sci. Techn. – Électrotechn. Et Énerg., **67**, *2*, pp. 93–98 (2022).
24. M.A. Mossa, H. Echeikh, A. Ma'arif, *Dynamic performance analysis of a five-phase PMSM drive using model reference adaptive system and enhanced sliding mode Observer*, Journal of Robotics and Control (JRC), **3**, *3*, pp. 289–308 (2022).
25. W. Liu, S. Sui, C.L.P. Chen, *Event-triggered predefined-time output feedback fuzzy adaptive control of permanent magnet synchronous motor systems*, Engineering Applications of Artificial Intelligence, **142**, pp. 109882 (2025).
26. P.Q. Khanh, H.P.H. Anh, *Advanced PMSM speed control using fuzzy PI method for hybrid power control technique*, Ain Shams Engineering Journal, **14**, *12*, pp. 102222 (2023).
27. F. Yang, M. Li, Y. Chen, Z. Chen, *Adaptive fuzzy command filtered control for asymmetric dynamic constrained nonlinear systems*, Communications in Nonlinear Science and Numerical Simulation, **142**, pp. 108513 (2025).
28. S. Moosakunju, S. Mini, V.P. Ushakumari, N. Mayadevi, R. Harikumar, *A hybrid fault detection and diagnosis algorithm for five-phase PMSM drive*, Arabian Journal for Science and Engineering, **48**, pp. 6507–6519 (2023).